

# TEM investigations of gate-all-around nanowire devices

P Favia<sup>1</sup> , O Richard, G Eneman, H Mertens, H Arimura, E Capogreco, A Hikavy , L Witters, P Kundu , R Loo , E Vancoille and H Bender 

Imec, Kapeldreef 75, 3001 Leuven, Belgium

E-mail: [paola.favia@imec.be](mailto:paola.favia@imec.be)

Received 28 June 2019, revised 10 September 2019

Accepted for publication 7 October 2019

Published 4 November 2019



## Abstract

Vertically stacked gate-all-around nanowires (GAA NWs) are considered a promising architecture for ultimately scaled complementary metal oxide semiconductor devices. These are the natural evolution of the fin-shaped field effect transistor (finFET) design and enable a better electrostatic control and a higher drive current per footprint w.r.t. previous architectures. Transmission electron microscopy (TEM) analysis is employed in the development stages of these devices to investigate morphology, material diffusion, oxidation and strain in order to achieve the desired nanowires shape and size and the required performances. Nano beam diffraction and geometric phase analysis of high-resolution scanning TEM (STEM) images are used in this work to evaluate strain at the nm-scale along the nanowires at different steps of the fabrication process. Initially strained Ge layers, in the early stages of the GAA NWs fabrication, relax after the fin-reveal and source/drain etching process steps. Strain is then restored after source/drain epitaxial deposition and maintained till the NWs release. TEM analyses of these structures are particularly challenging due to the dimensions of the GAA NWs which are smaller than the thickness of a typical TEM specimen. This generates artifacts due to different materials and multiple structures overlapping in projection in TEM images. To avoid these issues, several TEM lamellae at different positions in the device and/or 3D imaging STEM/energy dispersive spectroscopy tomography are employed.

Keywords: gate-all-around nanowires, transmission electron microscopy, strain, nano beam diffraction, tomography

(Some figures may appear in colour only in the online journal)

## Introduction

Gate-all-around nanowires (GAA NWs) are promising channel structures for the future technology nodes and are being considered as suitable replacement for fin-shaped field effect transistors (finFET). In fact, they offer a better electrostatic control than finFET [1] and are considered the ultimate complementary metal oxide semiconductor (CMOS) scaling device beyond the 7 nm technology node [2–5]. In the horizontal configuration they represent a natural extension of today's mainstream finFET architecture. The nanosheet stacking configuration, which is an extension of the vertically stacked NWs, can provide higher active volume per footprint than the finFET configuration [6].

The process flow to manufacture GAA NWs is similar to that of finFETs with the exception of a few additional steps. These steps, unique to the GAA fabrication, need special attention from the point of view of physical analysis to help improving the process. Due to the small dimensions at play, transmission electron microscopy (TEM) techniques need to be employed. Device size, roughness and interface sharpness are parameters that affect the electrical performance of GAA structures [7]. It is therefore important to monitor them along the process flow by standard TEM and/or scanning TEM (STEM) imaging. (S)TEM analysis has been in fact essential to reveal the smallest variation in NWs dimensions [8] as well as interface roughness. Recent advances in energy dispersive spectroscopy (EDS) detectors allow composition measurements with good accuracy and precision. The technique is mainly used in presence of materials that are not easily distinguishable in STEM

<sup>1</sup> Author to whom any correspondence should be addressed.

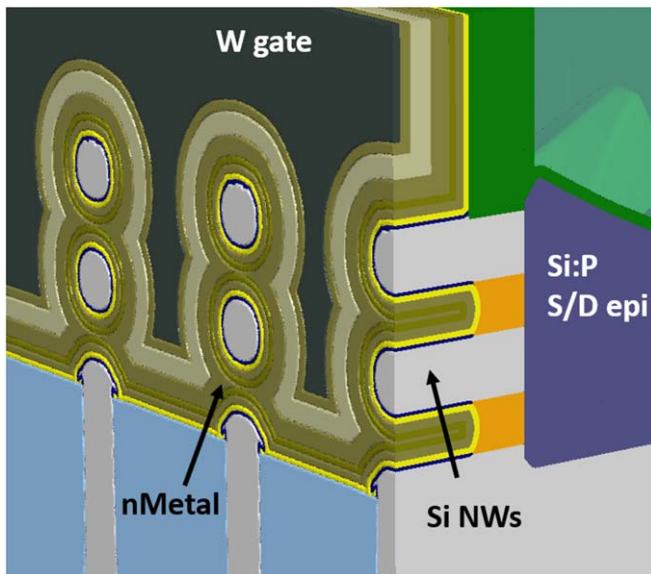


Figure 1. GAA NW device schematic (Coventor).

images [9] and to determine the presence of intermixing at the interfaces. These investigations may be hampered by overlap of different structures and materials in the TEM specimen thickness due to the 3-dimensional nature of the device with the nanowire dimensions being smaller than the thickness of a standard TEM specimen. Consequently, multiple TEM lamellae at different positions and different orientations (perpendicular to each other) or 3D tomographic analysis are necessary.

Strain is also an important parameter to monitor because it is directly linked to the carrier mobility of the devices [10, 11]. Besides TEM based techniques, strain in semiconductor devices can be measured by micro-Raman or high resolution x-ray diffraction (HRXRD). In the case of micro-Raman, structures such as GAA NWs are complicated to be resolved due to their short lengths. Only simple structures such as SiGe or Si fins without further processing of the gates or S/Ds can be measured and the interpretation of the results is not trivial [12]. HRXRD allows analysis of nm-scale confined volumes in terms of composition and strain [13] but the technique does not have the capability to distinguish single NWs. In order to learn how strain behaves in each single NW, TEM techniques are necessary. In recent years, several (S)TEM techniques have been developed. Nano beam diffraction (NBD) [14–16], precession NBD [17], high-resolution (S)TEM with geometrical phase analysis (GPA) [18, 19] and dark-field holography [20] are the most suitable to analyze strain in nano-devices. Strengths and weaknesses of these techniques are beyond the scope of this paper and have been thoroughly discussed elsewhere [21].

In this work, some of the unique to the GAA process flow steps are considered to illustrate the required TEM investigations and related challenges. Strain at the nanoscale is evaluated at different GAA manufacturing stages by NBD and GPA. Finally, 3D imaging and chemical analysis by STEM/EDS tomography is used to better analyze features and materials that are unclear due to projection overlap in standard TEM and STEM images.

## Experimental

The GAA NWs in this work are prepared at imec as part of the GAA NW process development. The process flow to fabricate the structures as shown in the schematic in figure 1 includes more than 150 steps. The main ones are summarized elsewhere for Si GAA NWs [6, 22]. A similar process flow is considered to fabricate Ge GAA NWs starting from a strain relaxed buffer (SRB) wafer [5, 23]. The GAA Si (or Ge) NWs process flow starts with ground plane doping in Si (Ge). Then, SiGe/Si (Ge)/SiGe/Si (Ge)/SiGe thin layers are epitaxially deposited. The SiGe layers are sacrificial layers that will be etched away later in the process to release the NWs. After fin patterning, shallow trench isolation (STI) oxide is deposited and etched till the base of the sacrificial layers to reveal the multilayered fins. After that, dummy gates and spacers are defined. Subsequently, embedded SiGe (Ge for Ge NWs) source/drain (S/D) is grown after spacer deposition and fin recess. After the removal of the dummy gates, the NWs are released by etching the SiGe sacrificial layers. The process flow ends with metal work function and metal contact deposition.

Thin TEM specimens of these structures at different process steps are prepared by focused ion beam (FIB) with common *in situ* lift-out methods. Standard TEM, STEM, EDS analysis, strain analysis and HAADF-STEM/EDS tomography are performed on a double corrected Titan<sup>3</sup> G2 60–300 instrument operating at 120 kV and equipped with a super-X EDS system (4 silicon drift detectors).

Strain analysis is done by either NBD measurements [14–16, 24] or by GPA analysis [25]. Nano beam diffraction patterns are acquired with a beam convergence of 0.18 mrad and a beam current of ~30 pA. The spatial resolution is 5–6 nm. The local strain maps or profiles are generated by comparing the diffraction spot positions in the relevant area with respect to a reference unstrained region using the Epsilon software from Thermo Fisher Scientific. Strain maps by GPA are generated using the script in Digital Micrograph (Gatan) from reference [25]. The analysis is applied to 2048 × 2048 pixels HAADF-STEM or annular-bright field (ABF)—STEM images. Stress simulations are performed using Sentaurus Process [26].

HAADF-STEM/EDS tomography is performed on a parallelepipedal pillar specimen [27] mounted on a Fischione 2050 on-axis rotation tomography holder. The volume of the pillar specimen in this work contains two fins (two sets of NWs) and S/D and one gate as indicated in the schematic in figure 2. HAADF-STEM images and EDS net counts maps series are automatically acquired tilting the specimen from −90° to +90° with increment of 3°. Such a tilt range would not be possible with a classical planar TEM sample for which the reduced tilt range would lead to reconstruction artefacts [20], as well as to elongation and different resolution in different slice orientations. Cross-correlation is used for the alignment of the HAADF-STEM images. The same alignment is applied to the EDS maps. The HAADF-STEM/EDS 3D reconstruction is obtained after applying the simultaneous iterative reconstruction technique (SIRT) algorithm with 20 iterations. Slices are then extracted from specific positions.

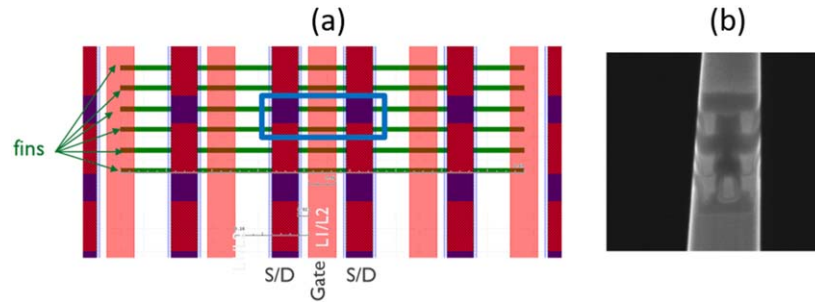


**Figure 2.** (a) Schematic of the fully processed structure used for HAADF-STEM/EDS tomography : the blue box is the intended volume of the pillar containing: 2 full fins and S/D contacts and 1 gate, (b) SEM image of the pillar sample viewed along the gate and S/D contacts.

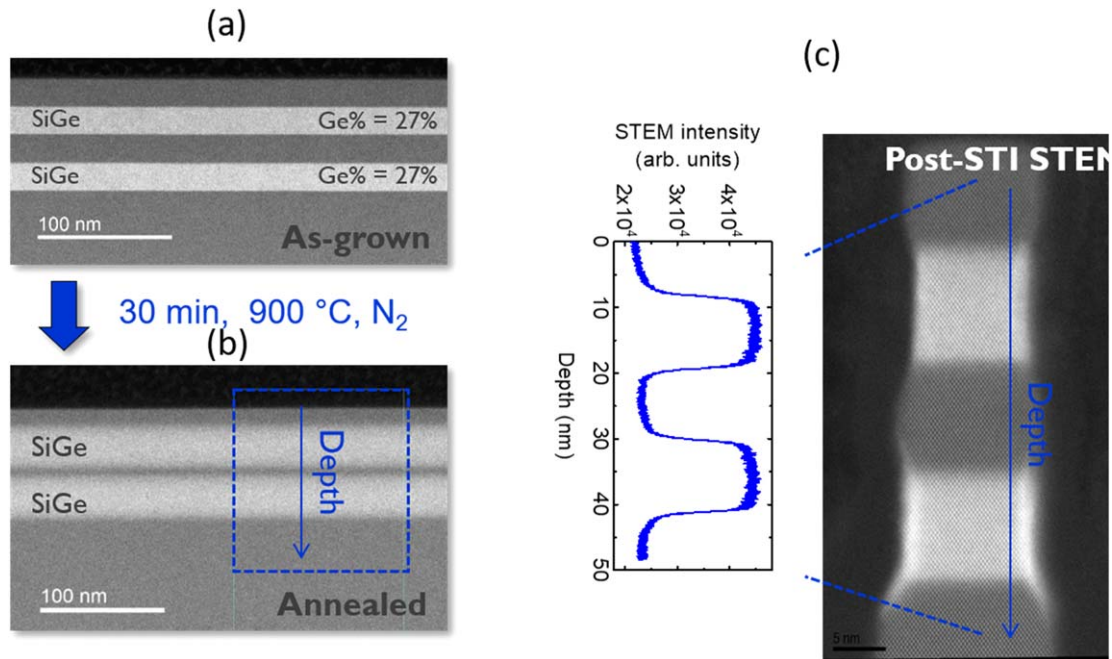


**Figure 3.** HAADF-STEM images of blanket SiGe/Si multilayer stack: (a) as grown, (b) blanket after 900 °C annealing, and (c) revealed Fin after 750 °C STI anneal. Reproduced with permission from *ECS Transactions* 77(5) (2017) Copyright 2017, The Electrochemical Society.

### Key process steps requiring TEM investigation

Most of the steps in the process flow for GAA NWs fabrication are identical to those for fins fabrication except for a few critical ones that require TEM investigation in the process development optimization. The steps unique to GAA NWs are, among others:

- SiGe/Si(Ge) multilayer epitaxial growth.
- Fins reveal with this multilayer stack.
- Nanowire release.

#### *Epitaxial multilayer deposition step for Si GAA NWs: interface sharpness and Si/Ge intermixing*

TEM investigation is required at this early step to check if the layers are sufficiently sharp to enable selective etching for the GAA processing, or if instead, the interfaces have broadened due to Si/Ge interdiffusion. It is observed that after annealing at 900 °C (as standardly used for STI oxide densification), the thickness of the SiGe sacrificial layers increases due to Ge diffusion into the Si layer, leading to a thinner Si layer and

therefore thinner wires later in the process flow. This effect needs to be minimized, and therefore should be monitored. Mertens *et al* found [28] a good agreement between SIMS and HAADF-STEM Ge profiles at the SiGe/Si interfaces in blanket samples. Therefore, HAADF-STEM intensity profiles can be used to monitor the Ge diffusion in the fins after oxide densification and fin reveal whereas SIMS analysis cannot be applied to such structures due to its lateral resolution (figure 3) [28]. As discussed in reference [28] a thermal budget reduction to 750 °C allows to suppress the Ge diffusion and to obtain interfaces with sharpness close to that in as-deposited layers.

#### *Fin reveal step in Si GAA NWs*

At this point of the process flow it is important to make sure that the fin sidewalls are smoothly etched across the multilayer stack and that there is no significant oxidation of the different materials on their sidewalls, while both sacrificial layers are fully exposed to be later etched to release the nanowires.

The oxidation issue has been discussed by Mertens *et al* [6]. A SiN liner deposited around the fin before the STI oxide fill,



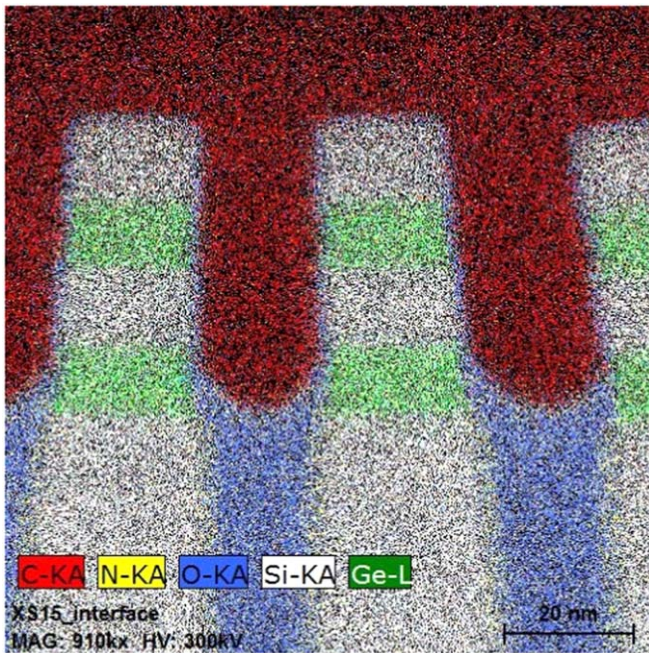


**Figure 4.** Overlaid EDS map after the Fin reveal step showing that the bottom SiGe layer is not fully revealed and hence the bottom Si wire will not be released later in the process.

helps in reducing the oxidation and controlling the shape and size of the fins.

TEM at this stage is very important to check that the multilayer fin is fully revealed, i.e. that the bottom sacrificial layer is exposed by fully removing the STI oxide next to it so that the layer can later be etched to allow the release of the nanowires. In figure 4 an example of a not fully revealed fin is shown in the EDS maps where the STI oxide is still covering the sidewall of the bottom SiGe. Also, an oxide layer is present at the sidewall of the fins for this structure.

#### Nanowire release Ge GAA NWs

At this step of the process flow TEM analysis is critical to check that the nanowires are well released. The view parallel to the wires does not give a clear and unambiguous answer, it is always best to check perpendicular cross sections viewing along the wires and gate as shown in figure 5. A criterion to judge if a nanowire is well released is by observing the profile of the high brightness dielectric material, in this case  $\text{HfO}_2$ : if the  $\text{HfO}_2$  encircles the nanowire, that means that it is released, if not, and the  $\text{HfO}_2$  profile appears open, then the nanowire is not released as it is the case for the bottom nanowire in figure 5(a). In this case, in the lateral view (figure 5(b)) a small imperfection of the  $\text{HfO}_x$  profile is visible but only in the cross-section perpendicular to the nanowires it is undoubtedly clear that the bottom right nanowire is not fully released.

#### Strain at different process steps—Ge GAA NWs

Lattice strain is an important parameter that influences the mobility of the carriers in the devices [10, 11]. Accurate

measurement of the strain requires referencing to an unstrained region in the same TEM specimen. Strain can be determined by the lattice difference of the region of interest (with lattice parameter  $d_{\text{ROI}}$ ) relative to a nominally unstrained reference region (with lattice parameter  $d_{\text{ref}}$ ), i.e.  $\frac{d_{\text{ROI}} - d_{\text{ref}}}{d_{\text{ref}}}$ . If the region of interest and the reference region consist of the same material, the formula yields directly the strain  $\varepsilon$  in the material while if the materials have different compositions, a relative lattice mismatch is obtained from which the effective strain can be calculated. In this paragraph, the strain evolution inside the Ge nanowires, throughout the subsequent process steps necessary to fabricate the Ge GAA NWs, is discussed. In particular, strain at the following steps is evaluated: (1) After multilayer deposition of blanket  $\text{SiGe}_{70}/\text{Ge}/\text{SiGe}_{70}/\text{Ge}/\text{SiGe}_{70}$  stack, (2) After fin reveal and S/D recess; (3) After S/D epi deposition and (4) After nanowire release. The notation used indicates  $\varepsilon_{xx}$  as in-plane strain along  $\langle 110 \rangle$  and  $\varepsilon_{zz}$  as strain along the growth direction  $\langle 001 \rangle$ . The reference region is taken in the unstrained SiGe buffer. Strain is determined either by NBD measurements or by post processing analysis by GPA of HR-STEM images.

- (1) A high resolution HAADF-STEM image of the as grown multilayer sample is shown in figure 6(a). The stack is composed by the Si substrate, a  $\text{SiGe}_{70}$  strain relaxed buffer and alternating  $\text{SiGe}_{70}$  and Ge layers of about 10 nm thick. The top is another  $\text{SiGe}_{70}$  layer. The corresponding strain maps, obtained by GPA,  $\varepsilon_{xx}$  along  $\langle 110 \rangle$  and  $\varepsilon_{zz}$  along  $\langle 001 \rangle$  are shown in figures 6(b) and (c) respectively. The top to bottom strain profiles  $\varepsilon_{xx}$  and  $\varepsilon_{zz}$ , integrated over the green window in figure 6(c), are displayed in figures 6(d) and (e) from experiments and TCAD calculations respectively. The  $\varepsilon_{xx}$  behavior (black curves) indicates that the lattice parameter of the Ge layers matches that of the SiGe relaxed buffer i.e. the Ge layers are biaxially strained. Experimental results and calculations are in good agreement.
- (2) NBD maps are acquired to evaluate the strain state after the fin reveal and S/D recess step (figures 7(a)–(c)). Model TCAD calculations are displayed in the inset in figures 7(b), (c). The NBD profiles in figure 7(d) show a relaxation of the Ge layers. These results are in qualitative agreement with TCAD simulations where a partial relaxation of these layers is observed.
- (3) After S/D deposition the strain is gained back as shown by NBD maps and corresponding profiles in figures 8(b)–(d). As also shown in the calculated maps (inset in figures 8(b), (c)) and corresponding profiles (figure 8(e)), due to geometrical factors the top Ge layer is less strained than the bottom one.
- (4) Finally, strain in released nanowires prior to RMG deposition, is obtained by GPA analysis of the HR-HAADF-STEM image in figure 9(a). Experiment and calculations (figures 9(b)–(e)) show that strain is still present in the nanowires after their release.

In conclusion, the initial strain in the Ge layers is lost after the fin reveal and S/D recess step but is gained back after S/D

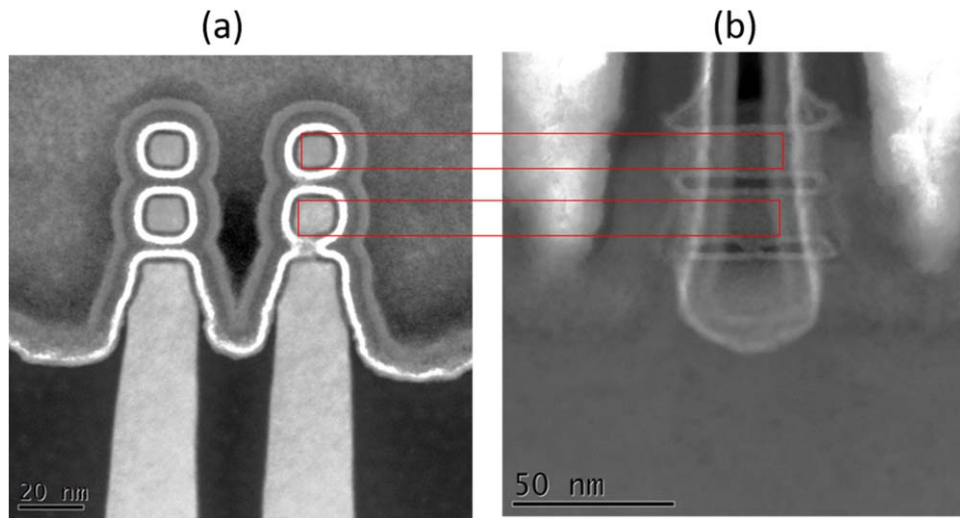


**Figure 5.** HAADF-STEM images of Ge NW device: (a) Cut across the fins and NWs, and (b) cut along the fins.

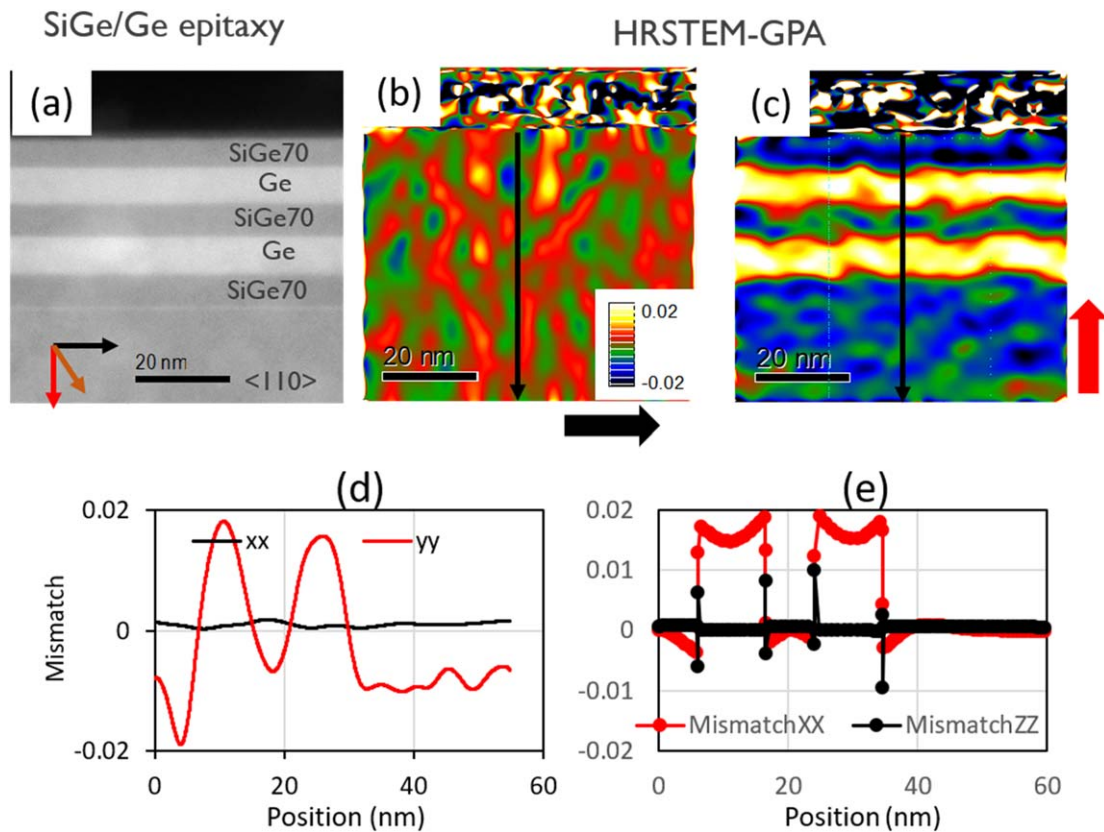


**Figure 6.** (a) HAADF-STEM of blanket multilayer SiGe<sub>70</sub>/Ge stack on SiGe<sub>70</sub> strain relaxed buffer, (b) HRSTEM-GPA xx, (c) HRSTEM-GPA zz. (d) GPA profile corresponding to figures 6(b) and (c) and (e) TCAD simulations profile from top to bottom.

deposition and maintained after nanowire release. Similar strain evolution was previously observed for single Ge GAA NWs [23].

### Challenges and solutions

Challenges encountered in TEM investigations of GAA NWs are mainly due to the dimensions of the nanowires (5–10 nm) being smaller than the typical thickness (30–50 nm) of a TEM

specimen. This engenders overlap in the thickness of the TEM lamella of multiple structures and materials as illustrated in figure 10. The volume used to prepare the lateral nanowires TEM lamella is indicated by the dotted box in the cross-section perpendicular to the NWs in figure 10(a). The resulting TEM specimen along the NWs is shown in figure 10(b). Overlap of multiple structures such as gate and NWs and contact and S/D is observed, as well as multiple materials in projection: W and Ge, SiGe (from S/D) and W (from contacts).



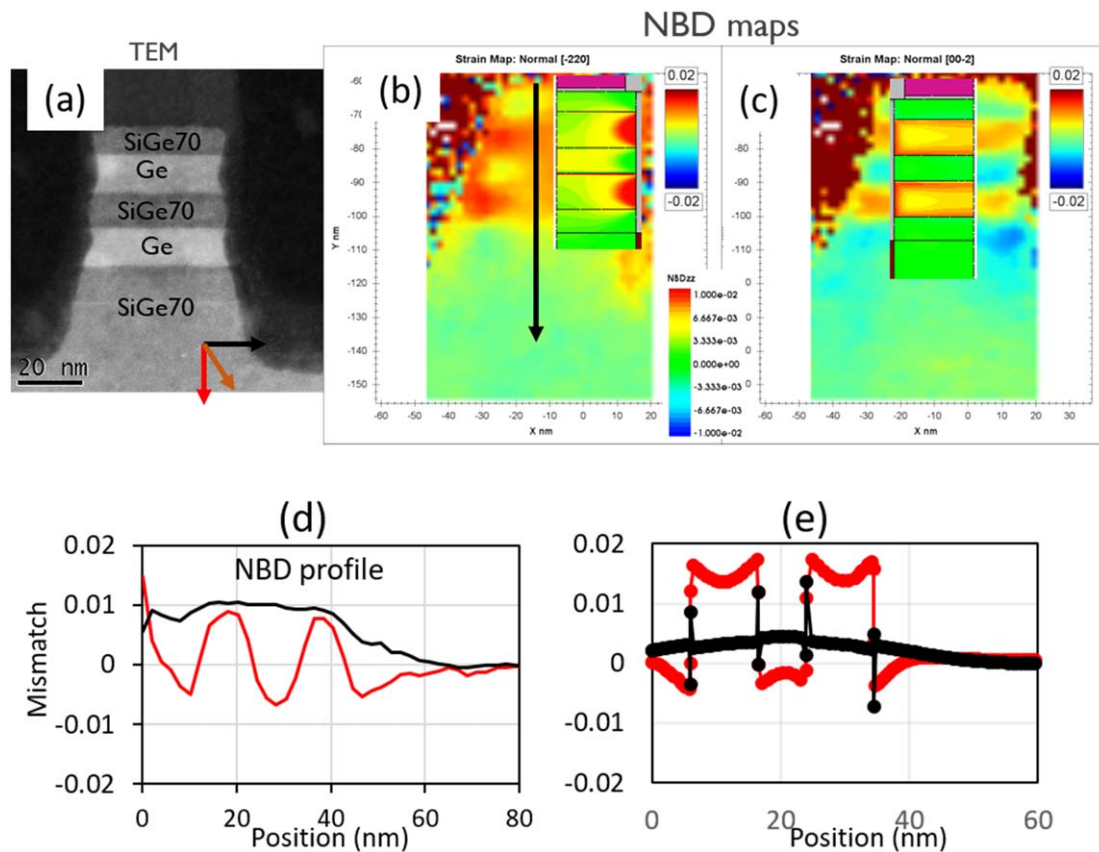


**Figure 7.** (a) HAADF-STEM of the multilayer stack after the ‘fin reveal’ step and S/D recess, (b) NBD map xx, (c) NBD map zz, simulations in the inset. (d) NBD profile of (b) along xx in black and along zz (map c) in red from top to bottom, (e) simulations profile along xx black and zz in red.

Another important issue to consider when investigating GAA devices is the tri-dimensionality of these structures. As shown in the schematic for a GAA device in figure 1, different structures are visible in the two perpendicular views and/or in the depth of the structure. This brings up the necessity of having more than one TEM lamella. In most cases, two, perpendicular to each other, ultrathin cross-sections are necessary to investigate shape, dimensions, strain etc in the across and along to the NWs direction and multiple cross sections at different depth in the device are also important to obtain information on different structures such as gates, contacts etc.

An alternative to acquiring images from multiple TEM lamellas and therefore multiple different devices, one for each TEM specimen, is the use of 3D analysis to gather information from a single unique device. Two main different approaches can be considered in a TEM: through focal imaging (TFS) methods such as confocal microscopy [29, 30], ptychography [31] HAADF-STEM and integrated differential phase contrast (iDPC) through focal series [32, 33], and STEM/EDS tomography [27, 34–36]. The TFS approach allows 2D high resolution imaging with 5–6 nm depth resolution. No chemical information is possible except that extracted from the HAADF-STEM contrast in the images. The STEM/EDS tomography approach allows probing of larger regions with a 3D resolution of 5 nm [27]. Chemical information is, in this case, provided by EDS analysis. Slices can be extracted from the reconstructed volume in any direction, including parallel the wafer surface,

with equal spatial resolution as alternative for the several ultrathin specimen approach.

### 3D imaging of GAA NWs by STEM/EDS tomography

HAADF-STEM/EDS tomography is applied on a fully processed Ge GAA NW device. The HAADF-STEM, Ge, Hf, O, Ti and W EDS slices extracted from the reconstructed volumes are shown in figures 11(b), (c) at the position of one of the fins and in the STI oxide spacing. The positions are marked on slice a (figure 11(a)) coming from the center of the gate (orange line in HAADF-STEM b image). It can be observed that the bottom nanowires are not fully released in this device. Consequently, these nanowires are not fully surrounded by the  $\text{HfO}_2$  layer exhibiting a bright contrast in the HAADF-STEM slice. This is also observed in the Ge and Hf EDS b slices obtained from the left fin where the bottom Ge and Hf signals are narrower than for the top nanowire which is fully released. This is observed for both fins (figures 12(c) and (e)). The TiN metallic barrier of the W contact and the TiAl layer of the replacement metal gate layers stack are detected in the Ti EDS slices.

The c slices (figure 11(c)) are extracted in the oxide spacing between the fins.

Artefacts like ghost contrasts of the gate between the fins (b HAADF-STEM slice) and weak O signal in the fin due to the silicon oxide between the fins (b O slice) are observed. These

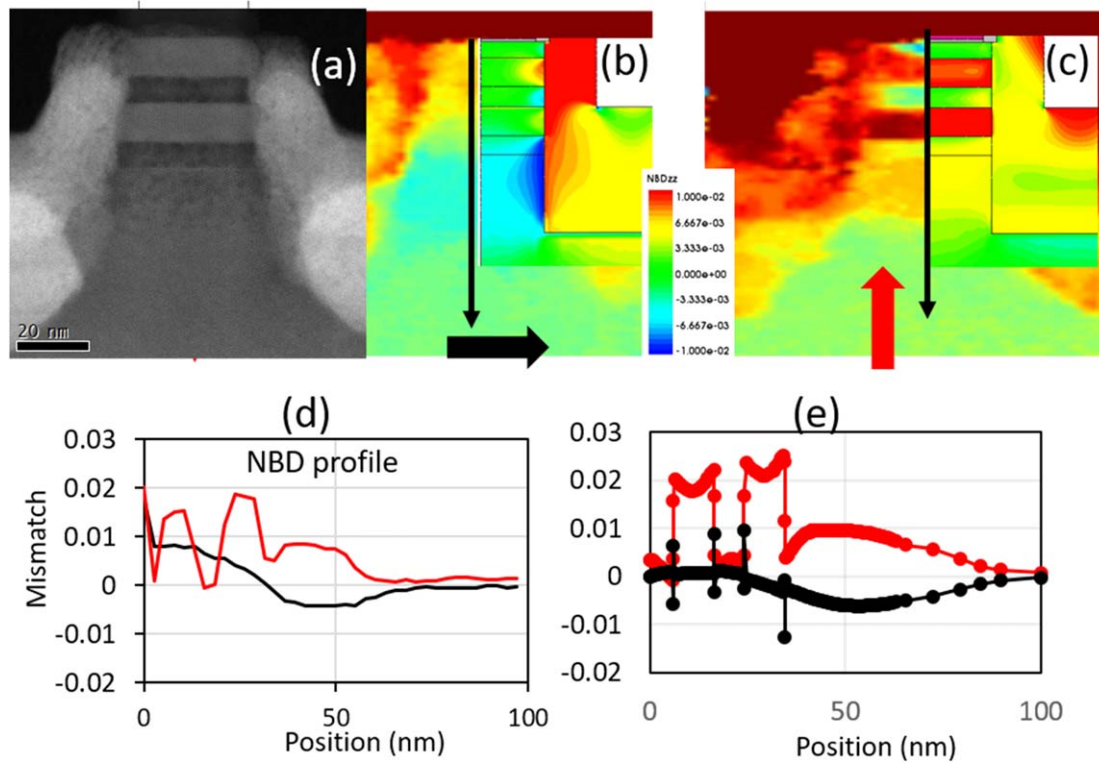


**Figure 8.** (a) HAADF-STEM of fin multilayer after S/D epitaxial Ge deposition, (b) NBD map xx, (c) NBD map zz with the corresponding simulations in the inset. (d) NBD profile from top to bottom along xx (black) and zz (red) corresponding to 8(b) and 8(c) maps respectively. (e) profiles deduced from the simulated maps in inset in 8(b) (black) and 8(c) (red).

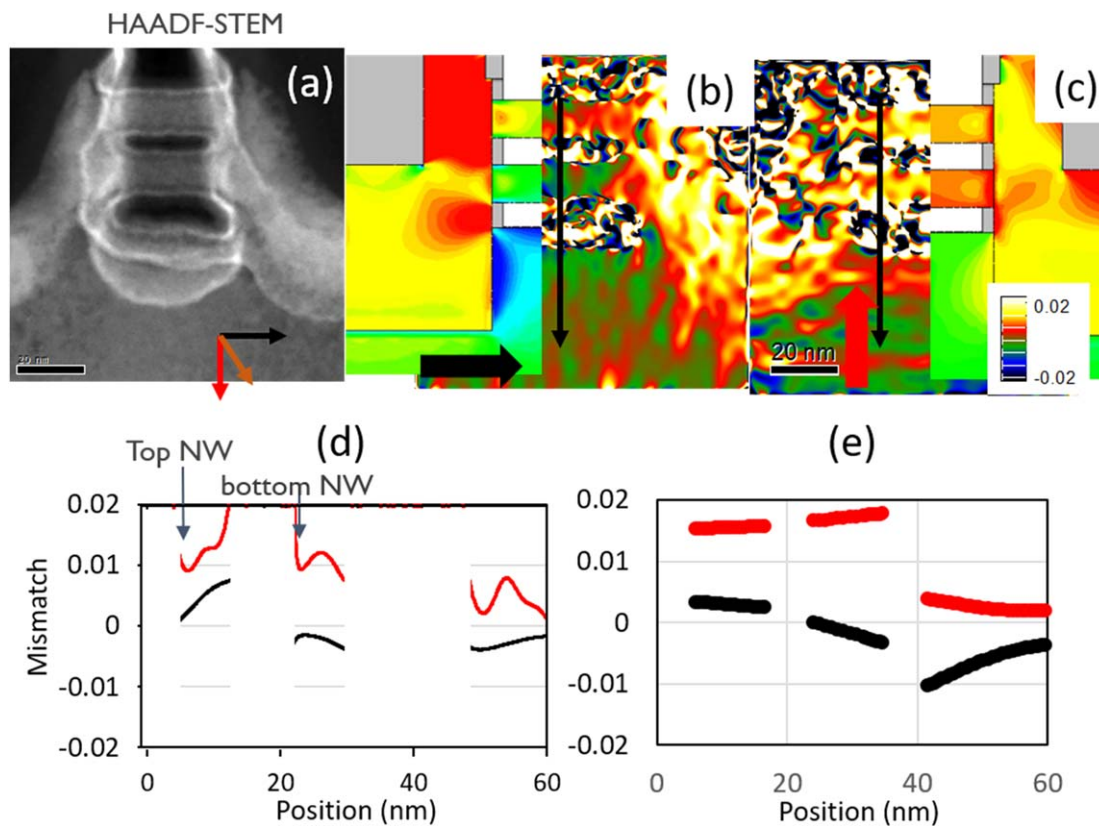


**Figure 9.** HAADF-STEM of released Ge GAA NWs prior to RMG deposition, (b) NBD and simulations (inset) map xx, (c) NBD and simulations (inset) map along zz. (d) NBD profile from top to bottom along xx (black) and zz (red) corresponding to 9(b) and 9(c) maps respectively. (e) simulations profiles from maps in inset in 9(b) (black) and 9(c) (red).

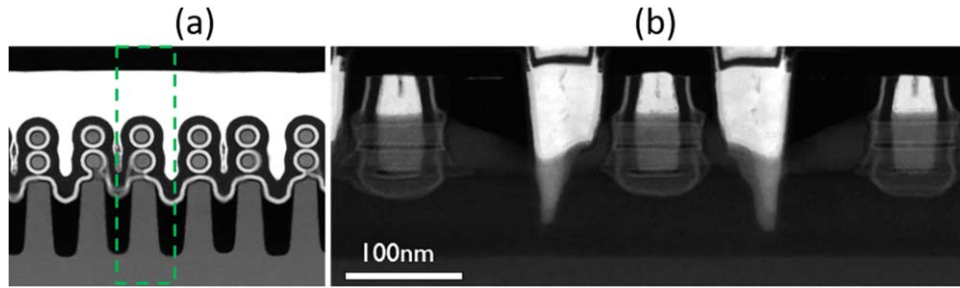


**Figure 10.** HAADF-STEM image of cross-section (a) across the GAA NWs and (b) along the GAA NWs. The dotted box represents the estimated volume of the sample parallel to the wires.

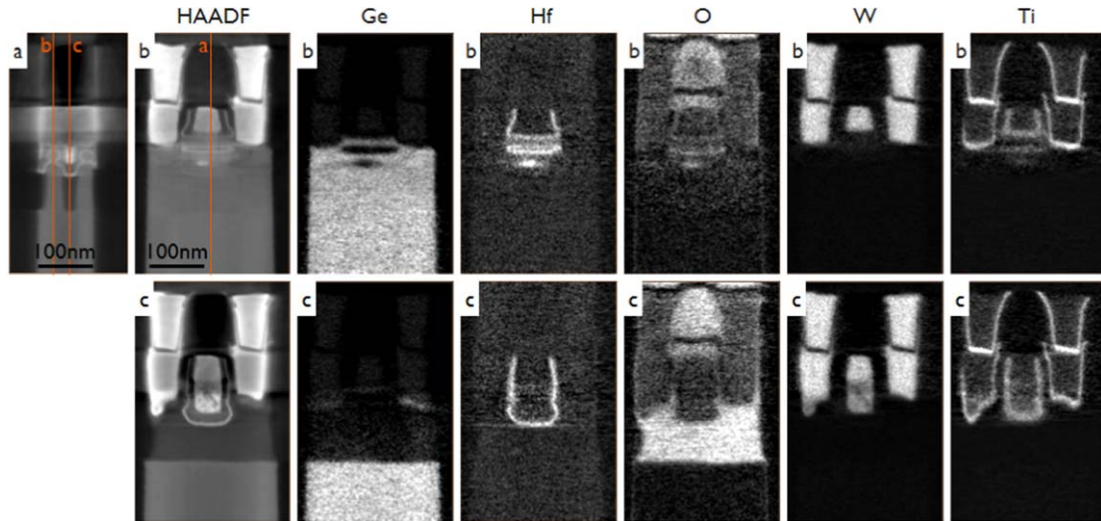


**Figure 11.** (a) HAADF-STEM tomography slice across the fins obtained by slicing through line a (b HAADF), (b) HAADF-STEM, Ge, Hf, O, W and Ti slices along the fin and wires obtained by slicing through line b (a), (c) HAADF-STEM, Ge, Hf, O, W and Ti slices between the fins and wires obtained by slicing through line c (a).

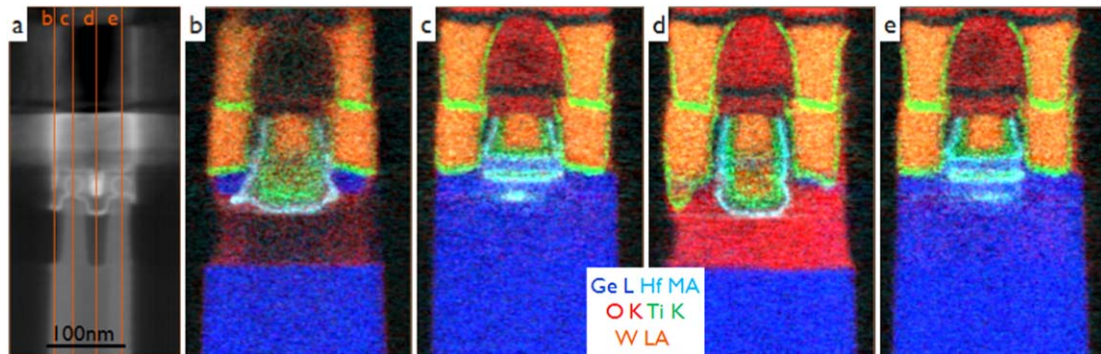


**Figure 12.** (a) HAADF-STEM tomography slice across the fins, and EDS tomography slices at the positions indicated in (a): slice b and d reveal strong differences of the shape of the gate between the fins. Slices c and e show that the bottom wire is only locally released.

artefacts are related to the resolution of the reconstruction. A more detailed discussion on the resolution and its dependence on the reconstruction conditions is presented in [27].

Slices combining the Ge, Hf, O, Ti and W signals and coming from different locations (figure 12(a)) are shown in the figures 12(b)–(e). The shape of the gate is different in the different spacings between the fins (figures 12(b), and (d)). In conventional 2D (S)TEM images and EDS maps, overlap in the thickness of the TEM specimen will occur and will render the interpretation of these images/EDS maps difficult.

STEM/EDS tomography is even more fundamental for the observation in a plane perpendicular to the growth direction. In fact, the preparation of plane-view TEM lamellas with FIB aiming at a particular layer or structure in the device suffers from several problems : as in a cross-section specimen materials overlap will occur in the thin slice, a small slope relative the growth plane is difficult to avoid and in general the interpretation of the SEM images during the FIB milling to determine on the endpoint position of the milling is less obvious. Tomography allows to extract the planar information easily at different heights



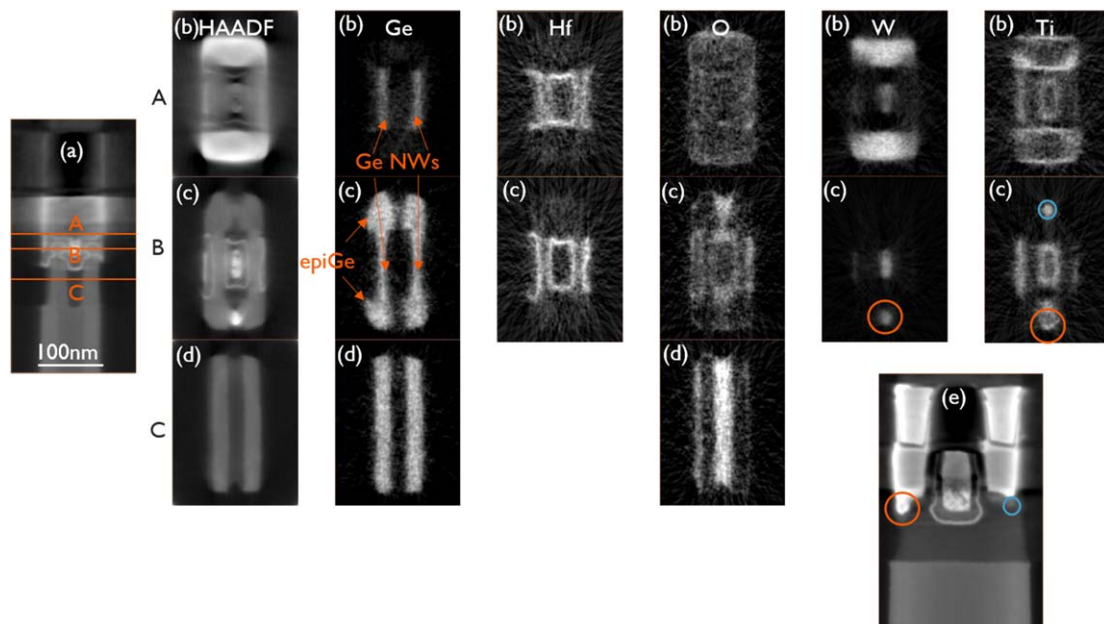


**Figure 13.** (a) HAADF-STEM tomography slice across the fins obtained by slicing through line a as marked on figure 11(b)-HAADF, (b)–(d) HAADF-STEM, Ge, Hf, O, W and Ti slices perpendicular to the growth axis obtained by slicing through the orange lines A (top wire), B (bottom wire) and C (bulk fins) in figure 13(a). The orange and blue encircled regions in the W and Ti slices in (c) correspond respectively to the left and right contacts in the HAADF-STEM image along the fins in figure 13(e) and highlight the non-uniform depth of the contact etch.

in the device as shown in figure 13. Important information that could affect the device performance can be extracted by observing these images. As an example, by comparing the Ge slices in figures 13(b) and (c) it is clear that the epitaxial Ge source and drain are barely present next to the top NWs while they are well connected to the bottom ones. The orange and blue encircled regions in the W and Ti maps in the c) slices correspond respectively to the left and right contacts in the HAADF-STEM image along the fins in figure 13(e) and they highlight the non-uniformity of the contact etch in the STI spacing.

## Conclusions

The process flows to fabricate GAA NWs and FINFETs are similar except for only a few additional steps unique to the GAA NWs preparation. GAA NW devices are being considered for future technology nodes. In this development stage it is important to investigate, by TEM, the new steps of the process flow for sharpness at interfaces, material diffusion, morphology, oxidation after STI fill and fin reveal, release of nanowires, and strain evolution.

The main challenges in these investigations are due to the small nanowire dimensions with respect to the thickness of a typical TEM specimen. In order to avoid overlap of materials and structures in the thickness of the TEM specimen, several ultrathin lamellas at different position and orientation in the device, are necessary. However, for each TEM specimen a different device is used, thus making the final information not very accurate since it is coming from different sources.

3D imaging is the alternative to the use of multiple TEM lamellas and devices. By extracting different slices from STEM/EDS tomography measurements it is possible to isolate different

structures in the device and distinguish the multiple elements in any slice orientation through the device volume.

## Acknowledgments

Patricia Van Marcke, Chris Drijbooms and Laura Nelissen are acknowledged for the FIB preparation.

The epitaxial layers have been grown in an ASM-Intrepid™. Air Liquide Advanced Materials is acknowledged for providing advanced precursor gases.

## ORCID iDs

P Favia <https://orcid.org/0000-0002-1019-3497>  
 A Hikavy <https://orcid.org/0000-0002-8201-075X>  
 P Kundu <https://orcid.org/0000-0003-2526-8372>  
 R Loo <https://orcid.org/0000-0003-3513-6058>  
 H Bender <https://orcid.org/0000-0003-0209-2597>

## References

- [1] Liebmann L, Zeng J, Zhu X, Yuan L, Bouche G and Kye J 2016 Overcoming scaling barriers through design technology CoOptimization 2016 *IEEE Symp. on VLSI Technology (Honolulu, HI, 2016)* 1–2
- [2] Kuhn K J 2012 Considerations for ultimate CMOS scaling *IEEE Trans. Electron Devices* **59** 1813–28
- [3] Yakimets D *et al* 2015 Vertical GAAFETs for the ultimate CMOS scaling *IEEE Trans. Electron Devices* **62** 1433–9

- [4] Shang H *et al* 2006 Investigation of FinFET devices for 32 nm technologies and beyond *Symp. on VLSI Technology, 2006. Digest of Technical Papers (Piscataway, NJ)* (IEEE) **54**–5 (<https://doi.org/10.1109/VLSIT.2006.1705213>)
- [5] Witters L *et al* 2017 Strained germanium gate-all-around pMOS device demonstration using selective wire release etch prior to replacement metal gate deposition *IEEE Trans. Electron Devices* **64** 4587–93
- [6] Mertens H *et al* 2017 Vertically stacked gate-all-around Si nanowire CMOS transistors with dual work function metal gates *Technical Digest—Int. Electron Devices Meeting, IEDM* **19.7.1–19.7.4**
- [7] IEEE 2017 International Roadmap for Devices and Systems 2017 Edition *IRDS*
- [8] Mertens H *et al* 2016 Gate-All-Around MOSFETs based on vertically stacked horizontal Si nanowires in a replacement metal gate process on bulk Si substrates *Digest Technical Papers—Symp. VLSI Technol.* 2016–September (<https://doi.org/10.1109/VLSIT.2016.7573416>)
- [9] Johanesen H, Strauss M, Kenslea A, Hakala C, Kwakman L, Boullart W, Mertens H, Siew Y K and Barla K 2019 Evaluation of the accuracy and precision of STEM and EDS metrology on horizontal GAA nanowire devices *Proc. SPIE* **109591C** 46
- [10] Krishnamohan T, Kim D, Dinh T V, Pham A, Meinerzhagen B, Jungemann C and Saraswat K 2008 Comparison of (001), (110) and (111) uniaxial- and biaxial-strained-Ge and strained-Si PMOS DGFETs for all channel orientations: mobility enhancement, drive current, delay and off-state leakage 2008 *IEEE Int. Electron Devices Meeting, San Francisco, CA* **4** 1–4
- [11] Eneman G *et al* 2012 Stress simulations for optimal mobility group IV p-and nMOS FinFETs for the 14 nm node and beyond 2012 *Int. Electron Devices Meeting* **131**–4
- [12] Nuytten T, Bogdanowicz J, Hantschel T, Schulze A, Favia P, Bender H, De Wolf I and Vandervorst W 2017 Advanced Raman spectroscopy using nanofocusing of light *Adv. Eng. Mater.* **19** 1–7
- [13] Schulze A *et al* 2017 Strain and compositional analysis of (Si) Ge fin structures using high resolution x-ray diffraction *Phys. Status Solidi C* **14** 1–7
- [14] Ozdol V B, Gammer C, Jin X G, Ercius P, Ophus C, Ciston J and Minor A M 2015 Strain mapping at nanometer resolution using advanced nano-beam electron diffraction *Appl. Phys. Lett.* **106** 253107
- [15] Béch   A, Rouvi  re J L, Barnes J P and Cooper D 2013 Strain measurement at the nanoscale: comparison between convergent beam electron diffraction, nano-beam electron diffraction, high resolution imaging and dark field electron holography *Ultramicroscopy* **131** 10–23
- [16] Favia P, Bargallo Gonzales M, Simoen E, Verheyen P, Klenov D and Bender H 2011 Nanobeam diffraction: technique evaluation and strain measurement on complementary metal oxide semiconductor devices *J. Electrochem. Soc.* **158** H438–46
- [17] Vincent R and Midgley P A 1994 Double conical beam-rocking system for measurement of integrated electron diffraction intensities *Ultramicroscopy* **53** 271–82
- [18] H  tch M J, Snoeck E and Kilaas R 1998 Quantitative measurement of displacement and strain fields from HREM micrographs *Ultramicroscopy* **74** 131–46
- [19] Rouvi  re J L and Sarigiannidou E 2005 Theoretical discussions on the geometrical phase analysis *Ultramicroscopy* **106** 1–17
- [20] H  tch M, Houdellier F, H  e F and Snoeck E 2008 Nanoscale holographic interferometry for strain measurements in electronic devices *Nature* **453** 1086–9
- [21] Cooper D, Denneulin T, Bernier N, B  ch   A and Rouvi  re J L 2016 Strain mapping of semiconductor specimens with nm-scale resolution in a transmission electron microscope *Micron* **80** 145–65
- [22] Ritzenh  ler R *et al* 2018 Vertically stacked gate-all-around Si nanowire CMOS transistors with reduced vertical nanowires separation, new work function metal gate solutions, and DC/AC performance optimization 2018 *IEEE Int. Electron Devices Meeting (IEDM) (San Francisco, CA, December)* **21.5.1–21.5.4**
- [23] Capogreco E *et al* 2018 First demonstration of vertically-stacked Gate-All-Around highly-strained Germanium nanowire p-FETs *IEEE Trans. Electron Devices* **65** 5145–50
- [24] Usuda K, Numata T, Irisawa T, Hirashita N and Takagi S 2005 Strain characterization in SOI and strained-Si on SGOI MOSFET channel using nano-beam electron diffraction (NBD) *Mater. Sci. Eng. B Solid-State Mater. Adv. Technol.* **124–125** 143–7
- [25] Koch C T FRWRtools plugin for Digital Micrograph based on ref. [18] ([https://www.physics.hu-berlin.de/en/sem/software/software\\_frwrtools](https://www.physics.hu-berlin.de/en/sem/software/software_frwrtools))
- [26] 2016 Synopsys TCAD simulator: Sentaurus Process Reference Manual M-2016, 12 (<https://www.synopsys.com/silicon/tcad/device-simulation/sentaurus-device.html>)
- [27] Bender H, Richard O, Kundu P, Favia P, Zhong Z, Palenstijn W J, Batenburg K J, Wirix M, Kohr H and Schoenmakers R 2019 Combined STEM-EDS tomography of nanowire structures *Semiconductor Science Technology* **34** 114002
- [28] Mertens H *et al* 2017 Gate-all-around transistors based on vertically stacked Si nanowires *ECS Trans.* **77** (Electrochemical Society Inc.) **19**–30
- [29] Einspahr J J and Voyles P M Prospects for 3D, nanometer-resolution imaging by confocal STEM *Ultramicroscopy* **106** 1041–52
- [30] Nellist P D, Cosgriff E C, Behan G and Kirkland A I 2008 Imaging modes for scanning confocal electron microscopy in a double aberration-corrected transmission electron microscope *Microsc. Microanal.* **14** 82–8
- [31] Gao S, Wang P, Zhang F, Martinez G T, Nellist P D, Pan X and Kirkland A I 2017 Electron ptychographic microscopy for three-dimensional imaging *Nature Commun.* **8** 163
- [32] Lazi   I, Bosch E G T, Yucelen E, Imlau R and Sorin L 2018 Thick (3D) sample imaging using iDPC-STEM at atomic scale *Microsc. Microanal.* **24** 170–1
- [33] Bender H, Bosch E G T, Richard O, Mendez D, Favia P and Lazi   I 2019 3D characterization of nanowire devices with STEM based modes *Semiconductor Science Technology* **34** 114001
- [34] Genc A, Kovarik L, Gu M, Cheng H, Plachinda P, Pullan L, Freitag B and Wang C 2013 XEDS STEM tomography for 3D chemical characterization of nanoscale particles *Ultramicroscopy* **131** 24–32
- [35] Fu B and Gribelyuk M A 2018 3D analysis of semiconductor devices: a combination of 3D imaging and 3D elemental analysis *J. Appl. Phys.* **123** 161554
- [36] Lepinay K, Lorut F, Pofelski A, Coquand R, Pantel R and Epicier T 2013 Defect analysis of a silicon nanowire transistor by x-ray energy dispersive spectroscopy technique in a STEM: 2D mappings and tomography *J. Phys. Conf. Ser.* **471** 012027